Effect of Arc Welding Electrode Temperature on Vapor and Fume Composition

N. T. Jenkins, Ph.D.
Massachusetts General Hospital, Charlestown, Massachusetts, USA

P. F. Mendez, Ph.D.
Colorado School of Mines, Golden, Colorado, USA

T. W. Eagar, Sc.D.
Massachusetts Institute of Technology, Cambridge, Massachusetts, USA

Abstract

Welding fume composition is dependent on the temperature at the surface of a GMAW electrode. This temperature varies with welding parameters and affects the amount, composition, and type of fume. A thermodynamic analysis based on the superheating expected at the surface of the molten electrode tip is presented to help understand observed fume composition.

Fume Composition

Efforts to reduce exposure to fume compounds by process control can be improved by better understanding how welding parameters affect the elemental composition of fume. Researchers have measured welding fume chemistry by many methods, but only a few have tried to predict the composition of the original vapor from thermodynamic calculations (1). The results of such modeling have been mixed, primarily because of incomplete assumptions about surface temperature, which is the primary factor that determines vapor composition (2).

Most fume researchers have assumed a single value for the gas metal arc welding (GMAW) droplet temperature to use in their thermodynamic calculations. Gray, et al., (3) and Podgaetskii, et al., (4) reported thermodynamic equilibria without explicitly stating the temperature they used. Hewitt & Hirst (5) considered fluxes in their calculations and Buki & Feldman (6) included oxides, but they too did not report the temperature. McAllister & Bosworth (7) assumed droplet temperatures were 1800–2200 K and were the first to include the effect of various shielding gases. Eagar, et al. (8) calculated gaseous equilibria for hexavalent chromium using varied shielding gases, at 2673 K.

None of these researchers considered the change in droplet temperature with time or how it changes with welding parameters. They also equated the surface temperature, which determines the composition of the evolved vapor and the fume formation rate, to the average temperature of the entire electrode droplet. They also did not consider that the surface temperature of the welding droplet during globular transfer was substantially different from that of a droplet during spray transfer (9). This can lead to misleading conclusions.

Electrode Temperature

Fume researchers have used simple approximations for the electrode temperature probably because determining the temperature of a material while welding is difficult. The transitory nature and extreme heat of welding prevents the use of thermocouples; calorimetric methods are also complicated to set up in situ and they do not provide an estimation of droplet surface temperature, but instead an average temperature for the whole droplet. The use of pyrometric techniques is problematic because the intense radiation from the arc overwhelms the infrared emissions of heated surfaces. Therefore many welding researchers rely on calculations of the weld metal temperatures.

The weld pool temperature is relatively simple to calculate. This has been performed several times, notably by Block-Bolten & Eagar (10) who found that because of evaporative heat losses, an upper limit of 2300K to 2800K exists for the temperature of the weld pool of steel gas tungsten arc welding (GTAW). However, for consumable electrodes in GMAW, the temperature of the welding droplet is more complicated to determine, because of an input of higher energy density, because of a more transitory nature (i.e. droplet detachment), and because measurements with which to compare the calculations are harder to obtain. Generally, values for the bulk temperature of the electrode are reported close to 2900K (11).

For GMAW, it should be noted that fume is dominated by evaporation from the electrode, which is consistent with how the temperature of the electrode tip is greater than that of the weld pool. Heile & Hill (12) and Sreekanthan (13) both compared the composition of fume collected during GMAW with an electrode of a different composition than that of the base plate and both found that the fume composition was determined almost entirely by the electrode. The authors performed a similar study considering production of hexavalent chromium, and found that the electrode is the predominant source of hexavalent chromium in GMAW fume (1).

Haidar (14–16), using a Cray supercomputer, performed a fundamental calculation of electrode droplet temperature and how it changes with time and welding parameters. The use of a supercomputer can be avoided if the droplet size is measured and a semi-empirical model created, like those in papers by Mendez, et al., (17) and Bosworth & Deam (18). A summary of such models can be seen in Fig. 1.

Although they may have greater bulk temperatures, smaller droplets, such as those formed during spray or pulsed transfer, have cooler surface temperatures than do larger droplets, like those from globular transfer, because there is a smaller barrier to heat transfer from the arc spot to the liquid-solid interface of the

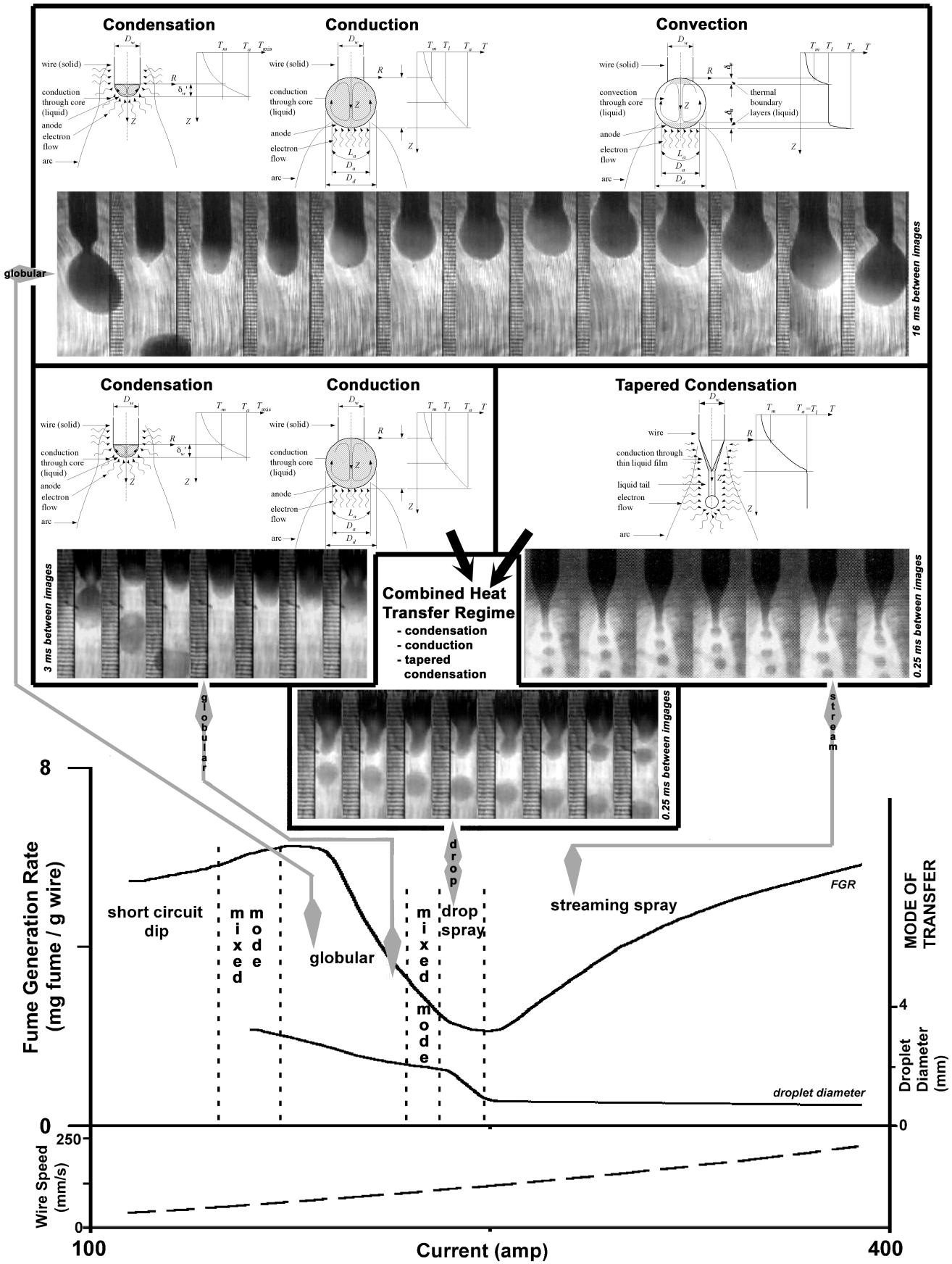

Figure 1: Heat transfer through GMAW electrodes is controlled by electrode droplet size (17). Shadowgraphs are from 2%O_2-Ar shielded GMAW with 1.6 mm mild steel electrode (19).

electrode (17). Therefore, conditions that create the smallest electrode droplet, and lower surface temperature, are the same as those that create fume containing the greatest fractions of volatile metals (e.g., manganese). Such conditions also minimize total fume formation. (Thus efforts to decrease fume formation rates with welding parameters may also increase the fraction of Mn in the fume, so Mn emission rates may not vary much.) The change in fume composition with droplet size can be extrapolated from how it varies with shielding gas oxidation potential, because that affects droplet size (15). An experiment with GMAW of ER308 stainless steel showed that the composition of fume varied with oxidation potential. (So as to prevent other possible sources of fume besides vaporization, such as from microspatter during droplet detachment, only a single electrode droplet was permitted to form at a time, by use of a single pulse of 100 amps for 500 ms.) See Fig. 2. Figure 3 contains similar results from another researcher. Previous researchers (12) have suggested that oxidation-assisted evaporation is why fume formation rate varies with shielding gas, but as stated before, the elemental composition of fume is dependent on the surface temperature of the weld metal, so the variation in composition with oxidation potential should be due to how electrode droplet size, and thereby surface temperature, varies with shielding gas (see Figs. 4 and 5). Current naturally also affects surface temperature. Figure 6 shows the direct correlation between fume formation rates and fraction of less volatile metals in fume; this indicates how surface temperature varies with current.

Superheat

The calculated energy balance of a GMAW electrode shows that the surface temperature of the electrode droplet may exceed the boiling point (17). Haidar (16) also calculated the surface temperature of a mild steel 1.2 mm GMAW electrode and compared it with the pyrometric measurement by Villeminot (23). Both found that the surface temperature at the tip of the electrode droplet was approximately 3100K. This is very close to, if not above, the boiling point of pure iron (values in the literature include 3025K (16), 3273K (24), 3121K (25)); it is certainly above the vapor-liquid transition for a typical iron alloy used in welding (Fig. 7).

In metallurgical processing, cooling by non-nucleate surface evaporation usually prevents superheating (10). However, with high-energy-density heat sources (i.e. electric arcs or lasers) and where heat loss is physically limited (like in thin GMAW electrodes), it is possible to inject energy into the system faster than it can be removed by evaporation, as calculated by the Langmuir equation with even the most conservative estimates (26). The Langmuir rate is for evaporation into a vacuum. When surrounded by an inert gas at atmospheric pressure, metal surfaces evaporate more slowly than the Langmuir rate, because the metal vapor must diffuse away from the evaporating surface. Thus evaporative cooling during welding is not as great as that predicted by the Langmuir rate. In any case, if an energy balance is to be maintained, the surface temperature, which controls vaporization and thus evaporative cooling, must increase until the conditions for balance are met. If the surface temperature exceeds the boiling point, superheating occurs.

Like other phase changes, boiling driven by superheat can occur through nucleation. Vapor bubbles usually form heterogeneously in crevices of the container that holds the boiling liquid. (Consider a boiling pot of water on a kitchen stove; the bubbles form on the bottom of the pot.) For bubbles to form, superheating must be present in order to overcome the activation energy required to create new surfaces. Because heat is usually added at the solid-liquid interface and lost at the gas-liquid interface, the amount of superheating depends on crevice size where vapor bubbles heterogeneously nucleate (27).

However, when a particle beam or electromagnetic radiation (e.g. electron condensation in arc welding) delivers heat, it does so at the gas-liquid interface. (For an experimental study of surface superheating, see Craciun & Craciun (28).) The solid-liquid interface is now where heat is lost and is therefore the coolest part of liquid. Thus vapor bubbles will not nucleate at solid crevices. Instead, the vapor phase must form bubbles completely in the liquid. Another difficulty for forming bubbles when intense heat is introduced at the liquid surface is that only a slender boundary layer will be hot enough for bubbles to nucleate in it. Under globular conditions, a 1.2 mm GMAW electrode droplet will have a thermal boundary layer approximately the size of 1/3 of the droplet or approximately 0.5 mm (17). Even if the convective core of the droplet were at the boiling point, the surface temperature of a steel electrode droplet would have to be greater than approximately 3200K for a bubble smaller than 0.5 mm in diameter to form, according to classical nucleation theory.

Richardson (29) states that classical nucleation predicts homogeneous superheats much greater than what is observed, but this is probably because the experimental measurements were made in liquids heated through the solid-liquid interface where crevices caused heterogeneous nucleation. This may also be the case for molten steel where vapor bubbles can presumably nucleate heterogeneously at defects in the liquid. Such would include pre-existing bubbles of gas, like carbon monoxide coming out of solution, which might explain why lower carbon content in steel electrodes is linked with lower fume formation rates (30-33). Other possible defects are miniscule inclusions of refractory impurities, the effect of which could be evaluated by creating solid GMAW wire containing a fine dispersion of high melting point particles, such as magnesia, which might provide more heterogeneous nucleation sites for more bubbles to form. When vapor bubbles encounter the liquid surface, they burst, creating spatter, or small droplets ejected from the metal surface (29). Therefore the amount of bubble formation could be detected by measuring the amount of spatter formed during welding.

Spatter small enough to remain airborne, dubbed microspatter, can contribute to fume. Such particles are similar in composition to that of the electrode. It has been claimed that globular fume has a greater portion of these “unfractionated” particles which would explain why fume formed during globular transfer has a lower fraction of the more volatile metals than does fume created during spray transfer at comparable currents (34). Using a cascade impactor, the authors found that

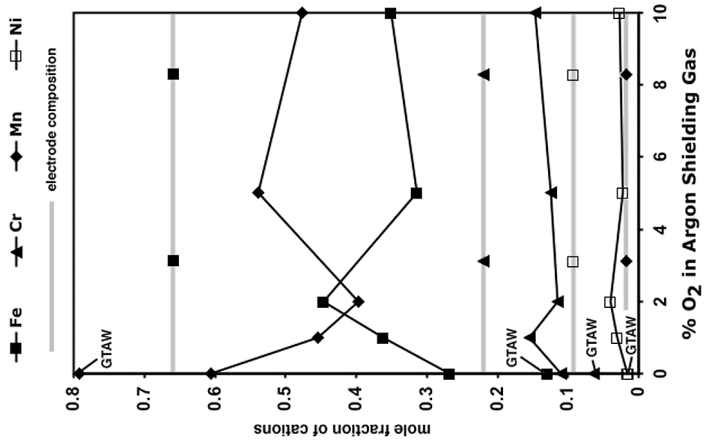

Figure 2: Oxidation potential effect on composition (ICPMS) of fume from single-pulse GMAW of ER308 stainless steel. GTAW fume composition from same weld metal also plotted. (Silicon is minutely present, but is not measureable by ICPMS)

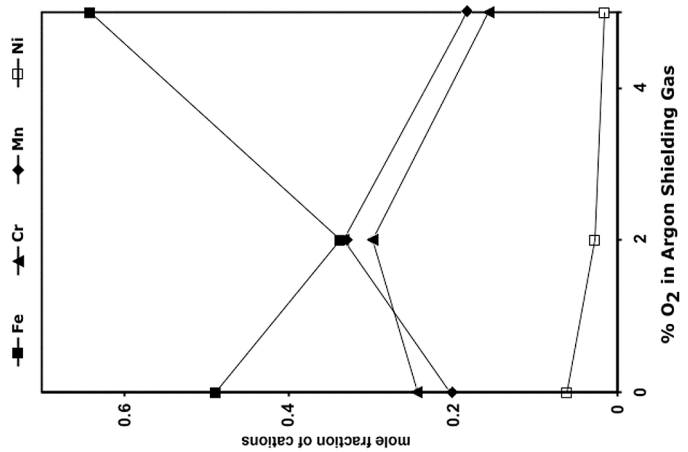

Figure 3: Fume composition (ICPMS) versus shielding gas oxidation potential in GMAW with 1.2 mm E308 stainless electrode, at 30V and 300ipm (13).

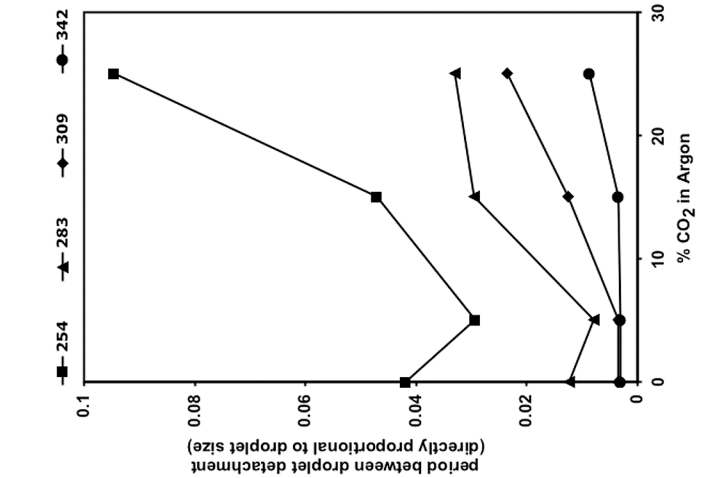

Figure 4: Electrode droplet period / droplet size versus shielding gas composition in 1.6mm mild steel GMAW for various currents (20).

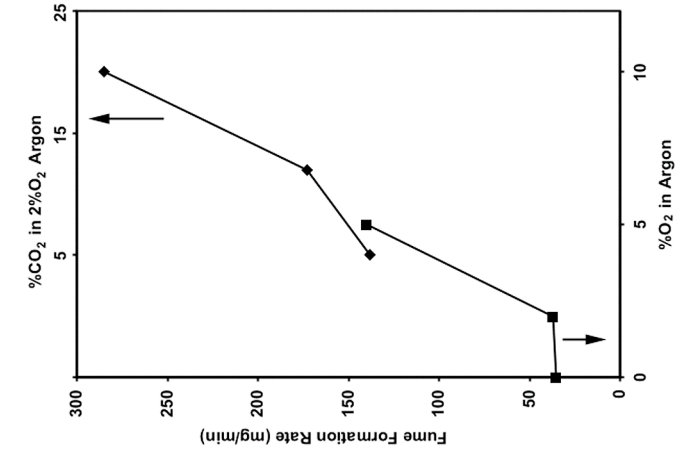

Figure 5: Fume formation rate dependence on shielding gas with 1.2 mm mild steel GMAW at 250 amp (12, 21).

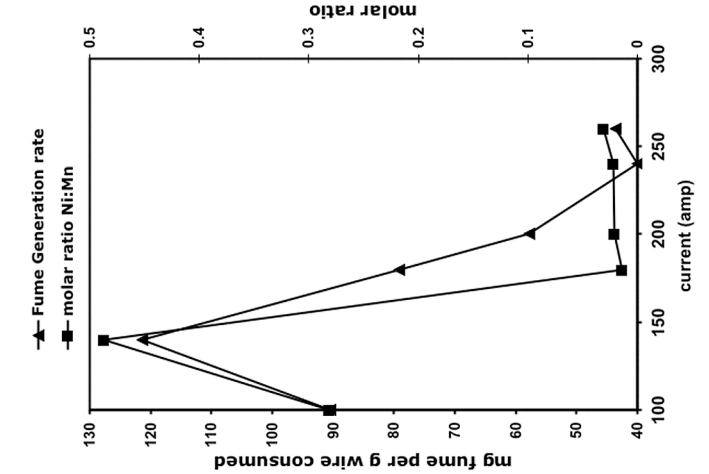

Figure 6a: Fume generation rate and Ni : Mn ratio versus current for argon shielded GMAW with 1.2 mm AWS ER307 Si electrode (22).

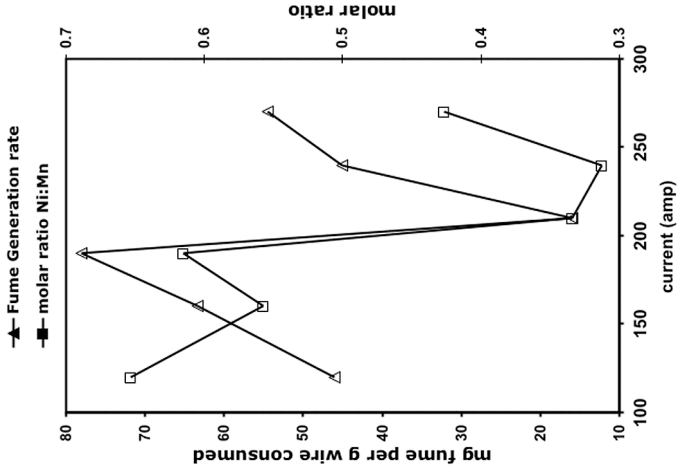

Figure 6b: Fume generation rate and Ni : Mn ratio versus current for argon shielded GMAW with 1.2 mm ER308L Si electrode (22).

less than 10% of GMAW fume by mass is microspatter. With an Aerosizer and SMPS, Zimmer, et al. (35) found that the mass of microspatter in GMAW fume was two orders of magnitude less than the mass of fume formed from vapor. The amount of microspatter is therefore too small to significantly affect the overall composition of GMAW fume. In addition, although the total fume formation rate is greater in globular transfer, the fraction of microspatter found in fume does not greatly change from spray transfer to globular transfer (1). Thus the variation in composition between the two modes must be due to a change in the vapor composition.

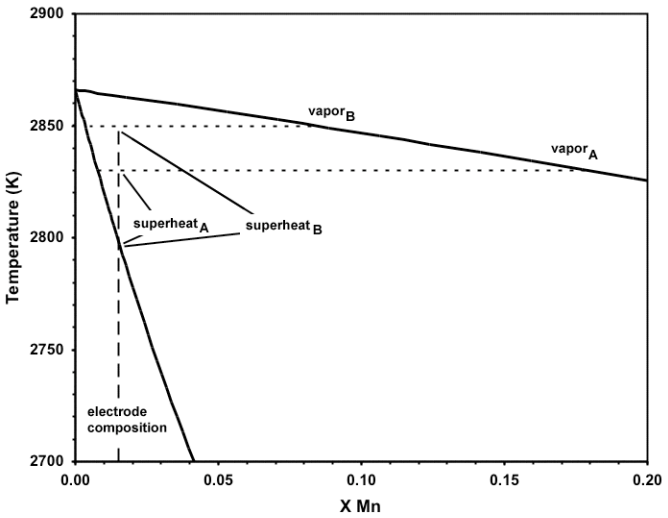

Figure 7: Fe-Mn vapor-liquid phase diagram at 0.3 atm., showing the effect of superheat on vapor composition (25).

The superheat, or amount by which the boiling point is exceeded, will determine the chemical composition of a multicomponent vapor, similar to how supercooling determines the composition of a condensate of an alloy. See Fig. 7, the Fe-Mn phase diagram at 0.3 atm., the approximate partial pressure of metal vapor in a GMAW arc (1). This is naturally a simple example of what can become complicated if one considers multicomponent alloys, the effect of halides on metal volatility (36), the presence of surface active elements (37), the effect of a plasma on vaporization (38), or mixing of the metal vapor with an oxidative environment (39). However, it demonstrates that even a small change in superheat can effect a large change in vapor composition, given the same initial composition of the liquid. This also explains how researchers have calculated that the vapor in a mild steel gas metal arc welding arc may be as much as half Mn, even though the wire contains less than 2 wt% Mn (30). In Fig. 7, it is shown how an increase of just 20K causes the vapor composition over a liquid containing 0.015 mole fraction Mn (typical in mild steel welding wire) to change from 0.18 mole fraction of Mn to 0.08 (typical amounts of Mn in welding fume, when reported as cation fraction (1).) The difference in droplet surface temperature between spray and globular transfer, or between pulsing and straight current can easily be greater than 100K (16), so welding process parameters that change droplet size and droplet surface temperature will also change fume composition accordingly.

Conclusions

1. Fume formation is a complex process and thus it is important to use correct input variables when predicting the elemental composition of welding fume.

2. The elemental composition of gas metal arc welding fume is almost the same as the elemental composition of vapor coming from the electrode.

3. Vaporization is controlled by surface temperature.

4. The surface temperature of GMAW droplets significantly varies with time, with mode and size, and with process. This has been modeled in prior literature, which should be referenced when selecting the temperature for thermodynamic calculations of fume composition.

5. This change in droplet surface temperature explains why welding fume composition changes with welding parameters that change metal transfer mode or droplet size.

6. Superheating can exist in GMAW electrode droplets.

7. The variation in fume composition with temperature can be seen in a Fe-Mn vapor-liquid phase diagram. Even a small temperature change (e.g. 20K) can have noticeable effect.

Acknowledgement

The funding for this project was provided by a grant from the U.S. Navy, Office of Naval Research.

References

1. N. T. Jenkins, *Chemistry of Airborne Particles from Metallurgical Processing*, Ph.D. Thesis, Massachusetts Institute of Technology, Cambridge, MA, (2003)

2. P. A. A. Khan and T. DebRoy, Alloying element vaporization and weld pool temperature during laser-welding of AISI 202 stainless-steel, *Metall. Trans. B*, 15, 641–644 (1984)

3. C. N. Gray, P. J. Hewitt, and R. Hicks, The prediction of fume compositions in stainless steel metal inert gas welding, *Proceedings of the Weld Pool Chemistry and Metallurgy International Conference*, N. Bailey, ed. Abington Hall, Cambridge, UK (1980)

4. V. Podgaetskii, A. Golovatyuk, and O. Levchenko, Mechanism of formation of welding aerosol and prediction of its composition in CO_2 welding. *Paton Weld. J.,* 1, 561–564 (1989)

5. P. J. Hewitt, and A. A. Hirst, Development and validation of a model to predict the metallic composition of flux-cored arc-welding fumes, *Ann. Occup. Hyg*., 35, 223–232 (1991)

6. A. A. Buki and A. M. Feldman, Prediction of composition of aerosol formed in welding in shielding gases, *Weld. Prod*., 27, 8–12 (1980)

7. T. McAllister, and M. Bosworth, Thermal mechanisms for the production of Cr(VI) [hexavalent chromium] in welding fume [in arc welding of stainless steels], *Australas. Weld. J.,* 44, 42–46 (1999)

8. T. W. Eagar, P. Sreekanthan, N. T. Jenkins, G. G. K. Murthy, J. M. Antonini, and J. D. Brain, Study of chromium in gas metal arc welding fume, *Proceedings of the Trends in Welding*, American Welding Society, Warrendale, PA (1998)

9. J. Ma, and R. L. Apps, MIG transfer discovery of importance to industry, *Weld. Met. Fabr.*, 9, 307–316 (1982)

10. A. Block-Bolton and T. W. Eagar, Metal vaporization from weld pools, *Metall. Trans. B*, 15B, 461–469 (1984)

11. O. Levchenko, Processes of welding fume formation (review), *Paton Weld. J.*, 8, 210–215 (1996)

12. R. F. Heile, and D. C. Hill, Particulate fume generation in arc welding processes, *Weld. J.*, 54, 201s–210s (1975)

13. P. Sreekanthan, *Study of Chromium in Welding Fume*, M.S. Thesis, Massachusetts Institute of Technology, Cambridge, Massachusetts (1997)

14. J. Haidar, A theoretical model for gas metal arc welding and gas tungsten arc welding, *J. Appl. Phys*., 84, 3518–3529 (1998)

15. J. Haidar, Predictions of metal droplet formation in gas metal arc welding. II, *J. Appl. Phys*., 84, 3530–3540 (1998)

16. J. Haidar, An analysis of heat transfer and fume production in gas metal arc welding. III, *J. Appl. Phys*., 85, 3448–3459 (1999)

17. P. Mendez, N. T. Jenkins, and T. W. Eagar, Effect of electrode droplet size on evaporation and fume generation in GMAW, *Proceedings of the Gas Metal Arc Welding for the 21st Century*, American Welding Society, Miami, Florida (2000)

18. M. R. Bosworth and R. T. Deam, Influence of GMAW droplet size on fume formation rate, *J. Phys, D Appl. Phys*., 33, 2605–2610 (2000)

19. L. A. Jones, T. W. Eagar, and J. H. Lang, Images of a steel electrode in Ar-2%O_2 shielding during constant current gas metal arc welding, *Weld. J.*, 77, 135s–141s (1998)

20. S. Rhee, and E. Kannateyasibu, Observation of metal transfer during gas metal arc-welding, *Weld. J*., 71, 381s–386s (1992)

21. D. E. Hilton, and P. N. Plumridge, Particulate fume generation during GMAW and GTAW, *Weld. Met. Fabr.*, 12, 555–560 (1991)

22. F. Eichhorn and T. Oldenburg, *Untersuchung der Scheissrauchentstehung beim Schweissen mit mittel- und hochlegierten Zusatzwerkstoffen*, DVS, Duesseldorf, BRD (1986)

23. P. Villeminot, Pyrometrie photographique appliquee au soudage. *Soudage et Techniques Connexes*, 21, 367 (1967)

24. Strem Chemicals*, Catalog No. 18*, p 418, Strem Chemicals, Newburyport, MA (1999)

25. B. Sundman, A program for performing thermodynamic calculations, *User Aspects of Phase Diagrams*, F. H. Hayes, ed., Institute of Metals, London, UK (1991)

26. J. D. Cobine and E. E. Burger, Analysis of electrode phenomena in the high-current arc, *J. Appl. Phys*., 26, 895–900 (1955)

27. G. F. Hewitt, J. M. Delhaye, and N. Zuber, eds., *Multiphase Science and Technology* Vol. 1. Hemisphere Publishing Corporation, Washington DC (1982)

28. V. Craciun, and D. Craciun, Does the subsurface superheating effect really exist? *Proceedings of the Advances in Laser Ablation of Materials Symposium*, R. K. Singh, D. H. Lowndes, D. B. Chrisey, E. Fogarassy, and J. Narayan, eds., Materials Research Society, Warrendale, PA (1998)

29. F. D. Richardson, *Physical Chemistry of Melts in Metallurgy*, Academic Press, London, UK (1974)

30. E. T. Turkdogan, P. Grieveson, and L. S. Darken, The formation of iron oxide fume, *J. Met*, 66, 521-526 (1962)

31. O. Grong, and N. Christensen, Factors controlling MIG weld metal chemistry, *Scand. J. Metall*., 4, 155-165 (1983)

32. T. Suga, and M. Kobayashi, Fume generation in CO_2 arc welding by flux-cored wire, *J. Japan Weld. Soc*., 2, 68-75 (1984)

33. S. E. Ferree, New generation of cored wires creates less fume and spatter, *Weld. J.*, 74, 45 (1995)

34. C. N. Gray, P. J. Hewitt, and P. R. M. Dare, New approach would help control welding fumes at source (MIG and MMA) part two: MIG fumes, *Weld. Met. Fabr.*, 10, 393–397 (1982)

35. A. T. Zimmer, P. A. Baron, P. Biswas, The influence of operating parameters on number-weighted aerosol size distribution generated from a gas metal arc welding process, *J. Aerosol Sci*., 33, 519-531 (2002)

36. D. A. Tillman, *Trace Metals in Combustion Systems*, Academic Press, San Diego, CA (1994)

37. P. Sahoo, M. M. Collur, and T. DebRoy, Effects of oxygen and sulfur on alloying element vaporization rates during laser-welding, *Metall. Trans. B*, 19, 967–972 (1988)

38. P. Sahoo, and T. DebRoy, Effect of low-pressure argon plasma on metal vaporization rates, *Mater. Lett*., 6, 406–408 (1988)

39. E. T. Turkdogan, P. Grieveson, L. S. Darken, Enhancement of diffusion-limited rates of vaporization of metals, *J. Phys. Chem.*, 67, 1647-1654 (1963)